frontiers | Frontiers in Water

TYPE Original Research
PUBLISHED 12 September 2022
DOI 10.3389/frwa.2022.996898

OPEN ACCESS

EDITED BY
Congsheng Fu,
Nanjing Institute of Geography and Limnology (CAS), China

REVIEWED BY
Pedro Maia Barbosa,
Université du Québec à Montréal, Canada
Alain Isabwe,
Institute of Urban Environment (CAS), China

*CORRESPONDENCE
Caroline Ganglo
carolineganglo20@gmail.com

SPECIALTY SECTION
This article was submitted to Water and Climate, a section of the journal Frontiers in Water

RECEIVED 18 July 2022
ACCEPTED 22 August 2022
PUBLISHED 12 September 2022

CITATION
Ganglo C, Manfrin A, Mendoza-Lera C and Lorke A (2022) Biocide treatment for mosquito control increases CH_4 emissions in floodplain pond mesocosms. *Front. Water* 4:996898. doi: 10.3389/frwa.2022.996898

Biocide treatment for mosquito control increases CH_4 emissions in floodplain pond mesocosms

Caroline Ganglo*, Alessandro Manfrin, Clara Mendoza-Lera and Andreas Lorke

Institute for Environmental Sciences, University of Koblenz-Landau, Landau, Germany

Shallow lentic freshwater aquatic systems are globally important emitters of methane (CH_4), a highly potent greenhouse gas. Previous laboratory studies indicated that bioturbation by chironomids can reduce CH_4 production and increase CH_4 oxidation by enhancing oxygen transport into sediment. Thus, reduction in chironomid density by application of biocides for mosquito control, such as *Bacillus thuringinesis* var. *israelensis* (Bti), have the potential to affect CH_4 emissions. We evaluated the effect of a 41% reduction in chironomid larvae abundance due to Bti applications on CH_4 dynamics in the aquatic and aquatic-terrestrial transition zones of 12 floodplain pond mesocosms (FPMs) (half treated, half control). We evaluated short-term (2 months) and seasonal effects by measuring CH_4 emissions, dissolved concentrations, and oxidation rates in spring, summer, autumn, and winter. On average, CH_4 emissions from the aquatic-terrestrial transition zone of the treated FPMs were 137 % higher than those of the control FPMs. The lack of differences in mean oxidation rates between the treated and control mesocosms suggests that a reduction in bioturbation and the associated decreased oxygen transport into the sediment promoted CH_4 production in the treated FPMs. Our findings point to potential effects of Bti on CH_4 biogeochemistry through alterations of the chironomid abundance, and highlight the underestimated role of invertebrates in biogeochemical cycling in these ecosystems.

KEYWORDS

Bti, biogeochemistry, methane, lentic shallow water, bioturbation

Introduction

Methane (CH_4) is a potent greenhouse gas, and the increase in its atmospheric concentration has been contributing about 23% of the additional radiative forcing accumulated in the lower atmosphere since preindustrial times (Etminan et al., 2016; Saunois et al., 2020). Nearly 50% of the total global CH_4 emissions are from aquatic ecosystems, with the largest contributions from small (<0.001 km^2) and shallow lentic aquatic system (Bergen et al., 2019; Rosentreter et al., 2021).

CH_4 is mainly produced by methanogenic archaea in anoxic sediments during the breakdown of organic matter (Segers, 1998). Its production rate is mainly controlled by redox conditions, quantity and quality of organic matter, and temperature (Yavitt et al., 1992; Peters and Conrad, 1996; Kelly and Chynoweth, 2014). On the other hand, CH_4 oxidation to carbon dioxide (CO_2) by methanotrophic bacteria under oxic conditions in sediment or in the water column is the major sink of CH_4 (Borrel et al., 2011). Up to 90% of the CH_4 produced can be oxidized before reaching the atmosphere as diffusive emission (Bastviken et al., 2004; Knoblauch et al., 2015; Sawakuchi et al., 2016). However, CH_4 oxidation in oxic aquatic compartments can be efficiently bypassed by non-diffusive emission pathways that directly transport CH_4 from anoxic sediments to the atmosphere, including bubble-mediated transport (ebullition) (Bastviken et al., 2004; Walter et al., 2007), and plant-mediated transport (Jeffrey et al., 2019; Bansal et al., 2020).

CH_4 production, oxidation, and emission (both diffusive and non-diffusive) in shallow aquatic systems are regulated by numerous factors, including water depth (Gorsky et al., 2019), the ratio of surface area to volume (Holgerson and Raymond, 2016), water temperature (Stadmark and Leonardson, 2005), sediment properties (Bodmer et al., 2020), system productivity (Delsontro et al., 2016), and vegetation (Bansal et al., 2020). The most overlooked processes affecting CH_4 dynamics are trophic and non-trophic interactions of methanogens and methanotrophs with benthic macroinvertebrates (Colina et al., 2021). In shallow, lentic ecosystems, benthic macroinvertebrate communities are often dominated by sediment-dwelling groups such as chironomid larvae (Diptera: Chironomidae) (Leeper and Taylor, 1998; Hölker et al., 2015). They construct U-shaped burrows (tubes) in areas of fine sediment (De Haas et al., 2006; Nogaro and Steinman, 2014), which they actively ventilate with surface water connecting the water column with anoxic sediment layers (Mclachlan and Cantrell, 1976; Hodkinson and Williams, 1980; Murniati et al., 2017). On the one hand, chironomids can promote CH_4 emissions by feeding on CH_4 oxidizing bacteria (Jones and Grey, 2011) and trigger the release of CH_4 gas bubbles (Booth et al., 2021). On the other hand, they may promote CH_4 oxidation by oxygenating the sediment (Kajan and Frenzel, 1999). Due to the seasonal variations in burrowing activity (Jackson and Mclachlan, 1991; Frouz et al., 2003), and the lack of *in situ* studies, it remains unclear how chironomid activity affects CH_4 dynamics at ecosystem scale (Kajan and Frenzel, 1999).

As most macroinvertebrates, chironomids are affected by anthropogenic stressors. A particular threat to chironomids are biological agents used to control larval stages of various nematocerous dipterans (i.e. black flies and mosquitoes) (Jakob and Poulin, 2016), such as *Bacillus thuringiensis* var. *israelensis* (Bti) (Boisvert and Boisvert, 2000; Brühl et al., 2020). Bti is widely used in Europe in in other parts of the world (Brühl et al., 2020). In Germany, up to 5000 tons of Bti formulations were applied to 400,000 ha in the Upper Rhine Valley between 1981 and 2016 (Becker et al., 2018). Due to its targeted effect on mosquitos and black flies, Bti is generally considered an "environmentally safe" alternative to traditional chemical pesticides (Brühl et al., 2020). Chironomid larvae were the most severely affected aquatic invertebrates and experienced abundance reductions by 50–87% in Bti-treated mesocosms and field studies in Germany (Allgeier et al., 2019a,b), which potentially also affects CH_4 dynamics in these ecosystems.

Here we tested whether the application of Bti has implications for CH_4 emission, concentration, and oxidation through reduction of the chironomid abundance. We measured dissolved CH_4 concentrations, CH_4 emission and oxidation rates from 12 floodplain pond mesocosms (FPMs), half of which were treated with Bti. A companion study carried out in parallel at the same FPMs revealed a reduction in chironomid larvae abundance in the treated FPMs by 41% compared to controls (Gerstle et al., 2022). We hypothesized that the reduced chironomid density would result in a decrease in CH_4 oxidation, higher concentrations of dissolved CH_4 in water, and in higher emissions to the atmosphere in the treated FPMs. We expected this effect to be most pronounced in the aquatic-terrestrial transition zone of the FPMs, which featured more favorable conditions for chironomids than the deeper areas of the FPMs with coarser sediment.

Materials and methods

Study site

The experiment was conducted in 12 identical FPMs, located at the Eusserthal Ecosystems Research Station in south-western (EERES; Germany 49°15'14" N, 7°57'42" E). The FPMs were constructed in 2018, have a surface area of $\sim$104 m^2 and can contain a water volume up to $\sim$25 m^3. The FPMs are separated from groundwater by a flexible rubber foil, can be fed on demand with water from the nearby stream, Sulzbach, and the water level can be adjusted to mimic flooding events (Stehle et al., 2022). Each FPM comprises a gradient in water depth with an aquatic-terrestrial transition zone (surface area: $\sim$30 m^2, water volume: $\sim$6 m^3, water depth: $\sim$0.20 m), and an aquatic zone (surface area: $\sim$43 m^2, water volume: $\sim$13 m^3, water depth: $\sim$0.30 m) (Supplementary Figure S1). The aquatic-terrestrial transition zone is characterized by a 15 cm thick layer of medium to coarse sand (diameter: $\sim$0.05 cm) and is covered by submerged macrophytes ($\sim$28 % areal coverage) and emerged plants ($\sim$46 %). In the aquatic zone, the bed consists of a 13 cm thick layer of coarse pebbles (diameter: $\sim$1-3 cm) and is colonized by submerged macrophytes (*Elodea* MICHX. and *Ceratophyllum* L. $\sim$35 % areal coverage), and by emergent plants (*Typha L.* $\sim$40 %) along the banks.

Experimental set-up

Flooding and Bti application

Following common practice of mosquito control applications at the Upper Rhine Valley, Bti was applied three times during elevated water levels (i.e., flooding) (Becker, 2006). Before each application, flooding was mimicked by gradually increasing the water level in all FPMs by 0.25 m (from 0.30 ± 0.02 m to 0.50 ± 0.02 m at the deepest location) over a period of two days (water level was continuously monitored in each FPM over the study period using pressure loggers (U20-001-03, Onset Computer Corporation, Hobo, USA). The water level was kept at high level for 10 days, before it was lowered over two days to its initial value. The flooding periods were from 11 to 22 April, 2 to 13 May, and 23 May to 3 June 2020 after which the water level slowly reduced to non-flooding levels over two days (see Supplementary Table S1 for more detail). On the third day of each flood, Bti was applied to every other FPM (*n*=6; referred to as treated FPMs in the following, Supplementary Figure S2). The untreated FPMs are considered as controls. Bti was applied as a suspension (VectoBac WG; Valent Biosciences, Illinois, USA) at maximum field rate (2.88 $\times$ 10^9 ITU ha^{-1} according to the manufacturer) using a knapsack sprayer (Prima 5, Gloria, Germany). The maximum field rate of Bti is usually applied when the water is deeper than 10 cm (Becker, 1997). The areal application rate (118 mg VectoBac® WG m^{-2}) was calculated using the surface area of the FPMs during flooding ($\sim$104 m^2). Bti granules quickly sink to the bottom of the pond (within an hour). Its ingredients and metabolites can therefore have accumulated in the treated ponds over the three applications.

Sampling design

To test the short-term effect of Bti applications, CH_4 emissions were measured 4 days before the first flooding (06 April 2020), and 3–5 days after each time the water level was decreased to its regular level (28 April, 14 May, 08 June) (Supplementary Figure S2). Dissolved CH_4 concentration was measured during seven sampling campaigns: 3 days before the first flooding (09 April 2020), 3–7 days after each Bti applications (20 April, 09 May, 28 May), and 3–5 days after each time the water level was decreased to its regular level (27 April, 14 May, 08 June).

To assess seasonal effects of Bti application, additional measurements of emissions and dissolved CH_4 concentrations were performed in spring (April 2020 and May 2020), summer (June 2020 and July 2020), autumn (September 2020 and November 2020), and winter (January 2020 and March 2021). In addition, a 2 days sampling campaigns in aquatic compartment of three FPMs (one treated FPM and two control FPMs) occurred in July (from 21 to 22) to assess daily variation in CH_4 emissions. These data were added to the summer measurement.

As a proxy for CH_4 oxidation, the isotopic signature of carbon in CH_4 ($\delta^{13}C$-CH_4) was measured in gas bubbles collected from the sediment and in dissolved gas in the surface water of the aquatic zone in May 2020 [2 days after the second Bti application (Spring)], June 2020 [2 days after the third flooding (Summer)] and in September 2020 (Autumn), as well as in February 2020 and March 2021 (Winter). Microbial CH_4 oxidation results in enrichment of ^{13}C in the remaining CH_4 (sampled in surface water) in comparison to freshly produced CH_4 (sampled as bubbles) (Bastviken et al., 2002).

CH_4 emissions

CH_4 emissions to the atmosphere were measured in both the aquatic and aquatic-terrestrial transition zones using transparent, floating, static chambers made of plastic polyethylene foil (allflex. E, 300µm, PA/EVOH/PA/PE, allvac Folien GmbH, Germany) (Supplementary Figure S3). Two chambers of different size were used to include vegetation: 72.5 cm x 72.5 cm x 54.6 cm and 72 cm x 72.5 cm x147.2 cm (LxWxH). Two battery-powered fans were placed inside each chamber to ensure uniform gas mixing. The chambers were connected in closed-loop with a gas analyzer (Ultra-portable Greenhouse Gas Analyzer; UGGA, Los Gatos Research Inc., Mountain View, CA, USA) using 2 m Tygon tubing. Relative humidity and temperature in the chamber was monitored *in-situ* (blueDan clima 4.0, ESYS GmbH, Berlin, Germany). Each chamber deployment lasted for about 5 min, or shorter if the relative humidity inside the chamber reached 90%.

CH_4 emissions were calculated based on the slope of a linear regression of the CH_4 mole fraction in the chamber headspace over time (S in ppm s^{-1})

$$F = S\left(\frac{V}{A}\right)\left(\frac{P}{RT}\right)t \tag{1}$$

where F represents the CH_4 flux (mmol m^{-2} d^{-1}), V is the chamber volume (m^3), A is the chamber surface area (m^2), p is atmospheric pressure (atm), R is the universal gas constant (0.0821 atm K^{-1} mol^{-1}), T is the temperature in the chamber headspace (K), and t is a unit conversion factor (t=86,400 s d^{-1}).

Dissolved CH_4

Dissolved CH_4 in the aquatic and aquatic-terrestrial transition zone was measured using the headspace method (International Hydropower Association, 2010). Water samples were collected at 5–10 cm depth using 1.2 l Schott glass bottles (sample volume: $\sim$0.9 l, headspace volume: $\sim$0.3 l) avoiding bubbling. Once closed, the bottle was vigorously shaken for 2 min to ensure gas equilibration between the water sample and the headspace. The bottle headspace was connected to a gas analyzer (Ultra-portable Greenhouse Gas Analyzer; UGGA, Los

Gatos Research Inc., Mountain View, CA, USA) in a closed-loop to measure the molar fraction of CH_4. Dissolved CH_4 in the water samples (c_{CH4} in μmol l^{-1}) was calculated as:

$$c_{CH4} = (X_{Final} - X_{Initial})(V_{HS}/V_s)(p/RT) + P_{Final}K_{CH4} \quad (2)$$

where X_{Final} and $X_{Initial}$ (in parts per million; ppm) are the mole fractions of CH_4 in the sample at equilibrium and the mole fraction of CH_4 in the atmosphere at the sampling time, respectively; V_{HS} and Vs (in l) are headspace volume and sample volume; K_{CH4} is the Henry coefficient of CH_4 (in mol l^{-1} atm^{-1}) at the sampling temperature T (in K); p is the atmospheric pressure (assumed constant at 1 atm) and R is the universal gas constant (0.0821 atm K^{-1} mol^{-1}). The temperature-dependent Henry coefficient was calculated following:

$$K_{CH4} = \left(\frac{\rho_w}{M_w}\right) \exp(-115.6477 + \frac{155.5756}{\frac{T}{100}} + 65.2533 \ln\left(\frac{T}{100}\right) - 6.1698\ T/100) \quad (3)$$

with ρ_w being water density (1,000 g l^{-1}) and M_w the molar mass of water (18.02 g mole^{-1}) (International Hydropower Association, 2010).

We also measured dissolved oxygen concentration and temperature using a multiprobe (WTW 82362 Weilheim, multi 3430 Germany) in the surface water of the aquatic and aquatic-terrestrial zone during the dissolved CH_4 concentration measurements.

CH_4 oxidative fraction

The carbon isotopic signature of methane ($\delta^{13}C$-CH_4) was determined from dissolved CH_4 in the surface water and from gas in the sediment. The gas dissolved in surface water was measured using the headspace method (water volume ~30 ml, headspace ~10 ml). The sediment surface was stirred to force ebullition and captured gas bubbles were collected using a handheld funnel. 2.5 ml of gas sample (both from headspace of the surface water and gas bubbles) was transferred to helium flushed exetainers (17 ml), which were analyzed using a PDZ Europa TGII trace gas analyzer and continuous on-line flow Europa 20/20 isotope ratio mass spectrometer (IRMS) at the Biology Center CASNa Sádkách Ceské Budějovice, Czech Republic. Isotopic data reported in δ units (‰) are relative to the Pee Dee belemnite (PDB) standard according to

$$\delta^{13}C = 1000(\frac{R_{sample}}{R_{standard}} - 1) \quad (4)$$

where R is the relative isotope abundance ratio $^{13}C/^{12}C$.

The fraction of CH_4 oxidized (f_{open}) was estimated using an open system, steady-state isotope mixing model (Leonte et al., 2017):

$$f_{open} = \frac{\alpha}{1-\alpha}\left(\frac{\delta_B + 1000}{\delta_{SW} + 1000} - 1\right) \quad (5)$$

where δ_{SW} and δ_B are the $\delta^{13}C$ values of dissolved CH_4 in surface water and in gas bubbles, respectively, α is the fractionation factor for aerobic CH_4 oxidation [$\alpha = 1.02$ (Bastviken et al., 2002)], and f_{open} is the fraction of the diffusive CH_4 flux from the sediment to the water column that becomes oxidized and is not emitted to the atmosphere. f_{open} was multiplied by 100 to obtain the CH4 oxidative fraction in percentage (%). As the model does not account for ebullition and plant-mediated emissions that bypass oxidation, the calculation may underestimate the fraction of the total CH_4 production that is oxidized. However, differences in estimates of the fraction oxidized between treatment and control FPMs can be considered as indicators for differences in oxidation rates.

We additionally calculated the oxidative fraction using the Rayleigh closed system model, which does not rely on steady-state conditions (Thottathil et al., 2018):

$$\ln(1-f_{close}) = \frac{\ln(\delta_B + 1000) - \ln(\delta_{SW} + 1000)}{\alpha - 1} \quad (6)$$

where f_{close} is the fraction of the diffusive CH_4 flux from the sediment to the water column that becomes oxidized and is not emitted to the atmosphere. f_{close} was multiplied by 100 to obtain the CH_4 oxidative fraction in percentage (%).

Statistical analysis

All data are reported as mean ± standard error. Short term changes in CH_4 emissions and dissolved CH_4 concentration were assessed with linear mixed effect models (LMEMs) using the lme function in the package nlme (Pinheiro et al., 2017) for R (R Core Team, 2013). The model included zone (aquatic and aquatic-terrestrial), treatment (treated and control FPMs), time (before the experiment started, at Bti applications and after Bti applications for dissolved CH_4; before the experiment started and after Bti applications for CH_4 emissions, Supplementary Figure S2), and their interaction as fixed factors. FPM number was used as random factor to account for repeated sampling. In both models, a backward selection was applied using likelihood ratio tests against reduced models following Zuur et al., 2010 chapter 5. The residuals of the initial and of the final selected model were assessed using qq-plots and model residual-fitted values plots. When necessary, dependent variables were log-transformed to meet normality and homogeneity of residual assumptions (Zuur et al., 2010). Potential serial correlation was also considered by fitting the initial model with different autocorrelation structures (Zuur et al., 2010) and using Akaike Information Criterion assessment to select the best model (Zuur et al., 2010). In case of significant effects of model interactions ($p \leq 0.05$), a contrast analysis was run using linear models with adjusted p-values after Benjamini-Hochberg correction to decrease false discovery rate due to multiple testing (Benjamini and Hochberg, 1995).

Longer-term (seasonal) effect of Bti application were assessed using LMEMs for CH_4 emissions, CH_4 dissolved concentrations and CH_4 oxidative fraction, similarly to the short-term analysis described above (short term analysis). Because sampling for CH_4 oxidative fraction started 2 days after the second Bti application, we analyzed these data for the long-term effect. For the longer-term effect, treatment, season (Spring (but excluding the time before the first Bti application) Summer, Autumn and Winter), and their interactions were considered as fixed factors and FPM as a random factor. The model selection and validation followed the same procedure as previously described.

Results

CH_4 emissions

During the short-term sampling, all FPMs were a source of CH_4 to the atmosphere with an overall mean emission of 4.06 ± 0.42 mmol m^{-2} d^{-1}. Before the Bti application, CH_4 emission was comparable among FPMs (Supplementary Table S3). During the Bti application period, CH_4 emissions did not differ between sampling times, treatment and zone (Supplementary Table S3; Figures 1A,B), except for a single sampling time (After Bti 2) (Figure 1B), when the emissions from the aquatic-terrestrial transition zone were higher in FPMs treated with Bti in comparison to the control FPMs (Tables 1, 2; Supplementary Table S4; Figure 1B).

CH_4 emissions after treatment were comparable among seasons and overall were consistently higher in the aquatic-terrestrial transition zone than in the aquatic one (Supplementary Table S3; Figures 1C,D). In the aquatic-terrestrial transition zone, we measured significantly higher CH_4 emissions from treated FPMs compared to the control units in spring, summer and autumn (Tables 1, 2; Supplementary Table S4; Figure 1D) (although slightly above significance). In the aquatic zone, CH_4 emissions were comparable between treatments and seasons (Table 1; Supplementary Table S4; Figure 1C).

Dissolved CH_4 concentrations

Overall, the FPMs were oxygen saturated with annual mean values of 98.0 ± 1.0% and mean annual temperature of 15.2 ± 0.3°C (Supplementary Figures S5, S6). All FPMs were supersaturated in dissolved CH_4 with respect to atmospheric equilibrium concentration throughout the year, with a mean saturation ratio of 6,311 ± 291%. Dissolved CH_4 was similar among FPMs before the first Bti application (Supplementary Tables S3, S4) and did not vary neither between treatment and control, nor between zones (Figures 2A,B). During the Bti application period (short-term sampling), dissolved CH_4 in surface water tended to increase and the concentration became significantly different from the previous times after the second Bti application (Supplementary Table S4). Seasonally, all FPMs had the highest dissolved CH_4 in summer (2.45 ± 0.20 μmol l^{-1}) and the lowest in autumn (0.85 ± 0.07 μmol l^{-1}) (Supplementary Table S4; Figures 2A,B).

CH_4 oxidative fraction

The average mixing ratio of CH_4 in gas bubbles was 12.7 ± 1.1 % and the $\delta^{13}C\text{-}CH_4$ in bubble gas (−61.1 ± 0.6 ‰) was consistently lower than in surface water (−48.8 ± 0.5 ‰) (Supplementary Table S2). Overall, 57–77 % and 45–53 % of the diffusive flux of CH_4 from the sediment was oxidized from the open system and closed system models, respectively (Supplementary Table S2). In some cases, oxidative fractions estimated using the open system, steady-state model were > 1 (in total 10 out of 48 samples). In those samples, $\delta^{13}C\text{-}CH_4$ values of surface water were strongly depleted (<-43 ‰). As $f_{open}>1$ indicates violation of the assumptions of isotope mixing model (Leonte et al., 2017), these data were not considered in the further analyses. Neither treatment nor season had a significant effect on the estimated CH_4 oxidative fractions from both models (Supplementary Table S3; Supplementary Figure S4).

Discussion

The present study is the first, to the best of our knowledge, to assess the biogeochemical implications of the application of the biocide Bti in floodplain pond mesocosms (FPM). We hypothesized that the reduced density of chironomids would lower CH_4 oxidation, leading to higher concentrations of dissolved CH_4 concentrations and emissions in treated FPMs, especially in the aquatic-terrestrial transition zone. In this zone, the CH_4 emissions from the treated FPMs were significantly higher during spring, summer and autumn compared to the untreated controls (Table 2). On average, the emissions from the aquatic-terrestrial transition zone were enhanced by 137 % during these samplings. This finding suggests a long-lasting effect of the application of Bti on chironomid density and therefore FPM CH_4 emissions, potentially related to reduction in chironomids. In a companion study (Gerstle et al., 2022) ∼41% less chironomid larvae were found in Bti-treated FPMs compared to control ones (Supplementary Figure S7; Supplementary Table S5) for an overview on collected taxa and

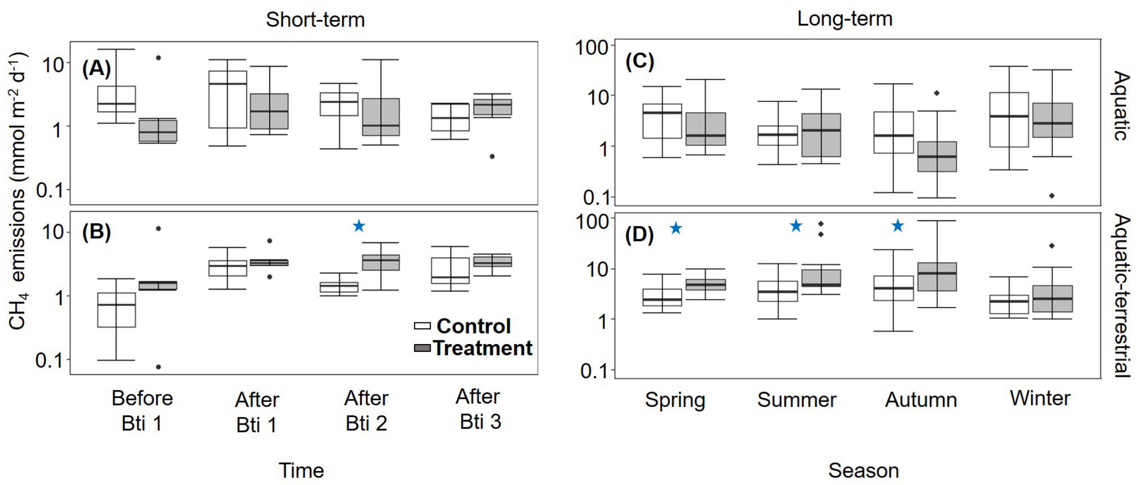

FIGURE 1
Box plots for CH_4 emissions ($n = 6$) measured in control (open boxes) and treated (filled boxes) FPMs. Data are presented for the short-term sampling during the Bti application period in the **(A)** aquatic and **(B)** aquatic-terrestrial compartments, and for the seasonal (long term) sampling in the **(C)** aquatic and **(D)** aquatic-terrestrial compartments. The lower and upper limits of the boxes show the 25th and 75th percentiles, respectively; the horizontal line inside the box is the median, and lower and upper whiskers show the 10th and 90th percentiles, respectively. Filled black circles are data falling outside the 10th and 90th percentiles. Blue stars denote significant difference between treated and control groups. Note that the *y*-axes are log-scaled.

TABLE 1 Significant effect of single factors and their interaction ($p \leq 0.05$) on dissolved CH_4 concentrations, emissions, and oxidative fraction (*F*-stat) after linear mixed effect model analysis.

Variables	Factors	numDF	denDF	F-value	*p*-value
CH_4 emissions -Short term	Zone × Treatment	1	82	5.88	0.02
CH_4 emissions -Seasonal	Zone	1	223	48.6	< 0.0001
	Zone × Treatment	1	223	16.80	0.0001
	Zone × Season	3	223	5.63	0.0001
CH_4 dissolved concentrations – Short term	Time	6	198	11.57	<0.0001
CH_4 dissolved concentrations – Seasonal	Season	3	349	38.30	<0.0001

numDF, numerator degrees of freedom; denDF, denominator degrees of freedom.
Full statistical report (including non-significant factors) available in Supplementary Tables S2, S3.

TABLE 2 Areal emission rates of CH_4 in the aquatic-terrestrial transition zone of untreated (Control) FPMs and those treated with Bti (Treatment), and the relative enhancement of CH_4 emissions from treated units.

FPMs	Control				Treatment			
Time/season	After Bti 2	Spring	Summer	Autumn	After Bti 2	Spring	Summer	Autumn
CH_4 emission (mmol m^{-2} d^{-1})	2.01 ± 0.26	3.10 ± 0.55	4.34 ± 0.59	5.43 ± 1.21	5.13 ± 1.00	5.26 ± 0.67	12.46 ± 4.71	12.97 ± 4.78
Relative enhancement in treated FPMs (%)	-	-	-	-	155	70	187	139

All numbers are presented as mean ± and standard error.

abundance). The chironomids in treated and control FPMs were sampled two weeks after our last CH_4 measurement, after the third and last application of Bti, in two different habitats: macrophytes and gravel, which respectively correspond to the aquatic-terrestrial and aquatic zone in our study. Chironomid larvae were by far the most abundant taxa and showed 72% higher abundance of all benthic macroinvertebrates' community (Gerstle et al., 2022).

Although our measurements cannot provide a causal relationship between observed changes in CH_4 emissions, in combination with the measured reduction in chironomid density, they support a previously hypothesized link between

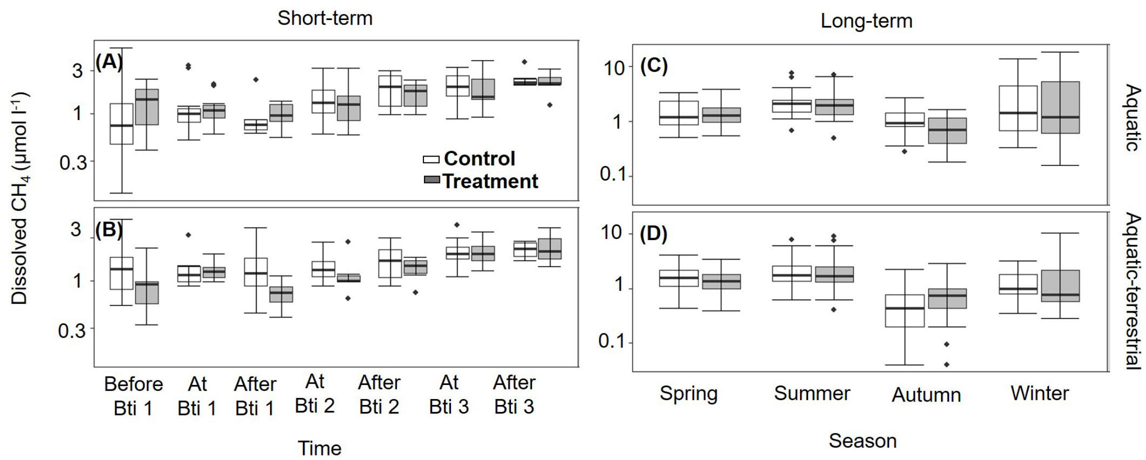

FIGURE 2
Box plots for dissolved CH_4 concentration ($n = 6$) measured in control (open boxes) and treated (filled boxes) FPMs. Data are presented for the short-term sampling during the Bti application period in the **(A)** aquatic and **(B)** aquatic-terrestrial compartments, and for the seasonal (long term) sampling in the **(C)** aquatic and **(D)** aquatic-terrestrial compartments. The lower and upper limits of the boxes show the 25th and 75th percentiles, respectively; the horizontal line inside the box is the median, and lower and upper whiskers show the 10th and 90th percentiles, respectively. Filled black circles are data falling outside the 10th and 90th percentiles. Note that *y*-axes are log-scaled.

chironomid abundance and CH_4 emissions (Hölker et al., 2015). Higher CH_4 emissions in Bti-treated FPMs were not detected immediately after Bti application, but in the long term. These findings might be explained by a different sensitivity to Bti depending on the chironomid developmental larval stage (Kästel et al., 2017). A stronger effect of Bti has been found in early instar chironomid larvae compared to mature larvae. As only mature larvae create burrows and thus bioturbate (Baranov et al., 2016), the reduction of mostly early instar larvae might explain why the effect on CH_4 dynamics was only detected when those larvae generations, after some time, developed the ability to burrow. Furthermore, we found that increased CH_4 emissions were only observed in the aquatic-terrestrial transition zone that is, in the area of the FPMs with finer sediment deposits (∼0.05 cm grain size) and abundant aquatic vegetation (mostly macrophytes). This area is the preferred habitat for tube dwelling chironomids (De Haas et al., 2006; Gerstle et al., 2022), while densities of chironomids in the gravel bed sediment (∼1-3 cm grain size) of the aquatic zone were much lower than in the aquatic-terrestrial transition zone (Supplementary Figure S7). The higher abundance of chironomids and their burrowing activity in the aquatic-terrestrial transition zone compared to the aquatic zone can explain why the effect was detected only in the aquatic-terrestrial transition zone. Finally, we observed significantly higher emissions during spring, summer and autumn, but not in winter, when the lower temperature (4 ± 0.4 °C) can have caused a decrease in chironomid metabolism (Jackson and Mclachlan, 1991; Frouz et al., 2003; Roskosch et al., 2012). All these results point toward an important role of chironomids in CH_4 dynamics and implications of Bti applications that are modulated by the sediment properties and the temporal dynamics of the chironomid population.

The exact mechanisms and processes by which the reduction in chironomid abundance may have caused the increase in emissions cannot be identified by our results, and remain an open question. We suggest a combination of trophic and non-trophic interactions of chironomids affecting CH_4 dynamics in FPMs, which is additionally influenced by FPM hydrodynamics: On the one hand, the increase of CH_4 emissions in the aquatic-terrestrial transition zone of treated FPMs was potentially caused by a reduction in grazing pressure on methane-oxidizing bacteria by chironomids, as observed by Kajan and Frenzel (1999) in laboratory experiments. On the other hand, the activity of the chironomids oxygenates the sediment, which reduces methanogenesis and promotes oxidation (Hölker et al., 2015; Murniati et al., 2017; Oliveira Junior et al., 2019; Booth et al., 2021), thus reducing CH_4 emissions as a consequence of non-trophic effects. However, this oxygenation pathway was not reflected in the oxidative fraction, which varied mainly as a function of the season, regardless of treatment. The dissolved CH_4 and oxygen concentrations were similar in both zones of the FPMs, indicating horizontal mixing of the surface water. Exchange flows and hydrodynamic conditions in small, shallow, and partially vegetated aquatic systems are expected to be governed by convective flows, which are generated by differential heating and cooling due to spatially varying water depths and light absorption properties of the water column and sediment surface (Nepf, 2012). Horizontal mixing of surface water in the FPMs may also have diluted differences in the isotopic signature of dissolved CH_4 and masked the identification of potential changes in CH_4 oxidation rates in the aquatic-terrestrial transition zone of the treated FPMs. With similar dissolved CH_4 concentrations and comparable hydrodynamic conditions, CH_4 emissions across the air-water interface can be expected to be of similar magnitude in both zones, suggesting that the higher emissions in the aquatic-terrestrial transition zone of the treated FPMs were supported by higher ebullition rates and/or plant-mediated emissions. As these emissions pathways mostly bypath CH_4 oxidation (Bastviken et al., 2004; Walter et al., 2007), their modification by chironomid activity would not necessarily be associated with changes in the isotopic composition of dissolved CH_4 nor in its concentration in surface water.

However, alternative mechanisms for the increase in CH_4 emissions from Bti treated FPMs that are not related to chironomid declines cannot be ruled out. Bti has been demonstrated to have long-lasting effects on the composition of microbial communities in the water column of microcosms that were treated with a high dose of Bti (about 10 times higher than the recommended field rate used in our experiments) (Duguma et al., 2015). Moreover, Bti is applied as a formulated suspension of toxin crystals, along with ingredients of unknown composition (Brühl et al., 2020). Parts of these ingredients, or their transformation products, may become available as a carbon source for methanogenesis. However, the applied areal rate of Bti application adds a relatively small amount of carbon. Assuming a carbon mass fraction in the Bti of about 50 % (as for sucrose), the total amount of applied Bti (3x 118 mg m^{-2}) would correspond to a total addition of 14.75 mmol C m^{-2}. This amount, if completely converted to CH_4, could fuel the average emission rate during spring (3.1 mmol m^{-2} d^{-1}, Table 2) for only 4 days, thus may not explain the enhanced emissions during summer and autumn.

The measurements analyzed in the present study provide only snapshots of the highly dynamic CH_4 emissions. Unresolved variations include diurnal changes in air-water gas exchange due to nocturnal mixing (Holgerson and Raymond, 2016; Poindexter et al., 2016), physiological activity of plants (Bansal et al., 2020), and episodically enhanced ebullition rates in response to atmospheric pressure changes (Walter et al., 2007; Maeck et al., 2014). Although the measured CH_4 emissions are in the range of fluxes reported for ponds in the temperate zone (Bergen et al., 2019; Peacock et al., 2021), the observed fluxes may not provide robust estimates of the overall CH_4 emissions from the FPMs due to the above-mentioned sampling limitations. Yet our findings indicate a potential effect of Bti application through chironomid reduction over extended periods and suggest seasonally enhanced ecosystem-scale CH_4 emissions by 137 %. In view of the widespread global use of Bti for mosquito control (Boisvert, 2005; Kästel et al., 2017), and the important role of the targeted aquatic ecosystems, such as lakes, ponds, FPMs, and freshwater wetlands, as the largest natural source of atmospheric CH_4 (Rosentreter et al., 2021), the effects at ecosystem scale need urgent evaluation in future studies. Additionally more detailed experiments that analyze the role of chironomids and other benthic invertebrates, and that of Bti in CH_4 dynamics at the sediment-water interface under controlled environmental or laboratory conditions are required.

Data availability statement

The data used to produce the results of this paper will be provided upon request.

Author contributions

CG: conceptualization, methodology, data collection, data curation, data analysis, and writing. AM: data analysis and writing. CM-L and AL: conceptualization, methodology, data analysis, and writing. All authors contributed to the article and approved the submitted version.

Funding

This work was funded by the Deutsche Forschungsgemeinschaft (DFG, German Research Foundation) —326210499/GRK2360, Systemlink.

Acknowledgments

We acknowledge the support of Rossano Bolpagni, Verena Gerstle, Sara Koblenschlag, Housam Ismaeli, Christoph Bors, Eliana Bohorquez Bedoya, and Sandhya Magesh during the planning and implementation of the experiment. Carsten A. Brühl provided valuable comments on earlier drafts of the manuscript. We thank the two anonymous reviewers for their comments that improved the manuscript.

Conflict of interest

The authors declare that the research was conducted in the absence of any commercial or financial relationships that could be construed as a potential conflict of interest.

Publisher's note

All claims expressed in this article are solely those of the authors and do not necessarily represent those

Supplementary material

The Supplementary Material for this article can be found online at: https://www.frontiersin.org/articles/10.3389/frwa.2022.996898/full#supplementary-material

References

Allgeier, S., Friedrich, A., and Brühl, C. A. (2019a). Mosquito control based on Bacillus thuringiensis israelensis (Bti) interrupts artificial wetland food chains. *Sci. Total Environ.* 686, 1173–1184. doi: 10.1016/j.scitotenv.2019.05.358

Allgeier, S., Kästel, A., and Brühl, C. A. (2019b). Adverse effects of mosquito control using Bacillus thuringiensis var. israelensis: reduced chironomid abundances in mesocosm, semi-field and field studies. *Ecotoxicol. Environ. Safety* 169, 786–796. doi: 10.1016/j.ecoenv.2018.11.050

Bansal, S., Johnson, O. F., Meier, J., and Zhu, X. (2020). Vegetation affects timing and location of wetland methane emissions. *J. Geophy. Res. Biogeosci.* 125, 1–14. doi: 10.1029/2020JG005777

Baranov, V., Lewandowski, J., and Krause, S. (2016). Bioturbation enhances the aerobic respiration of lake sediments in warming lakes. *Biol. Lett.* 12, 8–11. doi: 10.1098/rsbl.2016.0448

Bastviken, D., Cole, J., Pace, M., and Tranvik, L. (2004). Methane emissions from lakes: Dependence of lake characteristics, two regional assessments, and a global estimate. *Global Biogeochem. Cycles* 18, 1–12. doi: 10.1029/2004GB002238

Bastviken, D., Ejlertsson, J., and Tranvik, L. (2002). Measurement of methane oxidation in lakes: A comparison of methods. *Environ. Sci. Technol.* 36, 3354–3361. doi: 10.1021/es010311p

Becker, N. (1997). Microbial control of mosquitoes: management of the upper rhine mosquito population as a model programme. *Parasitol. Today* 13, 485–487. doi: 10.1016/S0169-4758(97)01154-X

Becker, N. (2006). Biological control mosquitoes: Management of the upper rhine mosquito population as a model programme. Eilenberg, J., and Hokkanen, H. M. T., editors. *An Ecological and Societal Approach to Biological Control.* New York, NY: Springer. p. 227–245.

Becker, N., Ludwig, M., and Su, T. (2018). Lack of resistance in aedes vexans field populations after 36 the upper Rhine Valley, Germany. *J. Am. Mosq. Control Assoc.* 34, 154–157. doi: 10.2987/17-6694.1

Benjamini, Y., and Hochberg, Y. (1995). Controlling the false discovery rate: a practical and powerful approach to multiple testing. *J. R. Stat. Soc. Series B* 57, 289–300. doi: 10.1111/j.2517-6161.1995.tb02031.x

Bergen, T. J. H. M., Barros, N., Mendonça, R., Aben, R. C. H., Althuizen, I. H. J., and Huszar, V., et al. (2019). Seasonal and diel variation in greenhouse gas emissions from an urban pond and its major drivers. *Limnol. Oceanogr.* 64, 2129–2139. doi: 10.1002/lno.11173

Bodmer, P., Wilkinson, J., and Lorke, A. (2020). Sediment properties drive spatial variability of potential methane production and oxidation in small streams. *J. Geophy. Res. Biogeosci.* 125, 1–15. doi: 10.1029/2019JG005213

Boisvert, M., and Boisvert, J. (2000). Effects of *Bacillus thuringiensis var.* israelensis on target and nontarget organisms: a review of laboratory and field experiments. *Biocont. Sci. Technol.* 10, 517–561. doi: 10.1080/095831500750016361

Boisvert, M. (2005). Utilization of *Bacillus thuringiensis var. israelensis* (Bti) - based formulations for the biological control of mosquitoes in Canada. *Victoria* 87–93.

Booth, M. T., Urbanic, M., Wang, X., and Beaulieu, J. J. (2021). Bioturbation frequency alters methane emissions from reservoir sediments. *Sci. Total Environ.* 789, 1–9. doi: 10.1016/j.scitotenv.2021.148033

Borrel, G., Jezequel, D., Biderre-Petit, C., Morel-Desrosiers, N., Morel, J-. P., and Pierre Peyret, G. F. (2011). Production and consumption of methane in freshwater lake ecosystems. *Res. Microbiol.* 162, 832–847. doi: 10.1016/j.resmic.2011.06.004

Brühl, C. A., Després, L., Frör, O., Patil, C. D., Poulin, B., and Tetreau, G., et al. (2020). Environmental and socioeconomic effects of mosquito control in Europe using the biocide Bacillus thuringiensis subsp. *israelensis (Bti). Sci. Total Environ.* 724, 1–16. doi: 10.1016/j.scitotenv.2020.137800

Colina, M., Meerhoff, M., Pérez, G., Veraart, A. J., Bodelier, P., and Horst, A., et al. (2021). Trophic and non- - trophic effects of fish and macroinvertebrates on carbon emissions. *Freshw. Biol.* 66, 1–15. doi: 10.1111/fwb.13795

De Haas, E. M., Wagner, C., Koelmans, A. A., Kraak, M. H. S., and Admiraal, W. (2006). Habitat selection by chironomid larvae: Fast growth requires fast food. *J. Anim. Ecol.* 75, 148–155. doi: 10.1111/j.1365-2656.2005.01030.x

Delsontro, T., Boutet, L., St-pierre, A., Giorgio, P. A., and Prairie, Y. T. (2016). Methane ebullition and diffusion from northern ponds and lakes regulated by the interaction between temperature and system productivity. *Limnol. Oceanogr.* 61, S62–S77. doi: 10.1002/lno.10335

Duguma, D., Hall, M. W., Rugman-Jones, P., Stouthamer, R., Neufeld, J. D., and Walton, W. E. (2015). Microbial communities and nutrient dynamics in experimental microcosms are altered after the application of a high dose of Bti. *J. Appl. Ecol.* 52, 763–773. doi: 10.1111/1365-2664.12422

Etminan, M., Myhre, G., Highwood, E. J., and Shine, K. P. (2016). Radiative forcing of carbon dioxide, methane, and nitrous oxide: a significant revision of the methane radiative forcing. *Geophys. Res. Let.* 12, 614–612, 623. doi: 10.1002/2016GL071930

Frouz, J., Matěna, J., and Ali, A. (2003). Survival strategies of chironomids (Diptera : Chironomidae) living in temporary habitats : a review. *Eur. J. Entomol.* 100, 459–465. doi: 10.14411/eje.2003.069

Gerstle, V., Manfrin, A., Kolbenschlag, S., Gerken, M., Mufachcher Ul Islam, A. S. M., Entling, M. H., et al. (2022). *Benthic macroinvertebrate community shifts induced by Bti also reduce Odonata emergence.* Environmental Pollution, Elsevier.

Gorsky, A. L., Racanelli, G. A., Belvin, A. C., and Chambers, R. M. (2019). Greenhouse gas flux from stormwater ponds in southeastern Virginia (USA). *Anthropocene* 28, 100218. doi: 10.1016/j.ancene.2019.100218

Hodkinson, I. D., and Williams, K. A. (1980). Tube formation and distribution of *Chironomus Plumosus L.* (Diptera : Chironomidae) in a eutrophic woodland pond. *Chironomidae*. 331–37. doi: 10.1016/B978-0-08-025889-8.50051-9

Holgerson, M. A., and Raymond, P. A. (2016). Large contribution to inland water CO2 and CH4 emissions from very small ponds. *Nat. Geosci.* 9, 222–226. doi: 10.1038/ngeo2654

Hölker, F., Vanni, M. J., Kuiper, J. J., Meile, C., Grossart, H. P., and Stief, P., et al. (2015). Tube-dwelling invertebrates: tiny ecosystem engineers have large effects in lake ecosystems. *Ecol. Monogr.* 85, 333–351. doi: 10.1890/14-1160.1

International Hydropower Association. (2010). *GHG Measurement Guidelines for Freshwater Reservoirs*. London: International Hydropower Association.

Jackson, J. M., and Mclachlan, A. J. (1991). Rain-pools on peat moorland as island habitats for midge larvae. *Hydrobiologia* 209, 59–65. doi: 10.1007/BF00006718

Jakob, C., and Poulin, B. (2016). Indirect effects of mosquito control using Bti on dragonflies and damselflies (Odonata) in the Camargue. *Insect Conserv. Divers.* 9, 161–169. doi: 10.1111/icad.12155

Jeffrey, L. C., Maher, D. T., Johnston, S. G., Kelaher, B. P., Steven, A., and Tait, D. R. (2019). Wetland methane emissions dominated by plant-mediated fluxes: Contrasting emissions pathways and seasons within a shallow freshwater subtropical wetland. *Limnol. Oceanogr.* 64, 1895–1912. doi: 10.1002/lno.11158

Jones, R. I., and Grey, J. (2011). Biogenic methane in freshwater food webs. *Freshw. Biol.* 56, 213–229. doi: 10.1111/j.1365-2427.2010.02494.x

Kajan, R., and Frenzel, P. (1999). The effect of chironomid larvae on production, oxidation and fluxes of methane in a flooded rice soil. *FEMS Microbiol. Ecol.* 28, 121–129. doi: 10.1111/j.1574-6941.1999.tb00567.x

Kästel, A., Allgeier, S., and Brühl, C. A. (2017). Decreasing Bacillus thuringiensis israelensis sensitivity of Chironomus riparius larvae with age indicates potential environmental risk for mosquito control. *Sci. Rep*. 7, 1–7. doi: 10.1038/s41598-017-14019-2

Kelly, C. A., and Chynoweth, D. P. (2014). The Contributions of Temperature and of the Input of Organic Matter in Controlling Rates of Sediment Methanogenesis. *Am. Soc. Limnol. Oceanography*, 26, 891–897. doi: 10.4319/lo.1981.26.5.0891

Knoblauch, C., Spott, O., Evgrafova, S., Kutzbach, L., and Pfeiffer, E. M. (2015). Regulation of methane production, oxidation, and emission by vascular plants and bryophytes in ponds of the northeast Siberian polygonal tundra. *J. Geophy. Res. Biogeosci.* 120, 2525–2541. doi: 10.1002/2015JG003053

Leeper, D. A., and Taylor, B. E. (1998). Insect emergence from a South Carolina (USA) temporary wetland pond, with emphasis on the Chironomidae (Diptera). *Chicago J.* 17, 54–72. doi: 10.2307/1468051

Leonte, M., Kessler, J. D., Kellermann, M. Y., Arrington, E. C., Valentine, D. L., and Sylva, S. P. (2017). Rapid rates of aerobic methane oxidation at the feather edge of gas hydrate stability in the waters of Hudson Canyon, US Atlantic Margin. *Geochim. Cosmochim. Acta* 204, 375–387. doi: 10.1016/j.gca.2017.01.009

Maeck, A., Hofmann, H., and Lorke, A. (2014). Pumping methane out of aquatic sediments andndash; Ebullition forcing mechanisms in an impounded river. *Biogeosciences* 11, 2925–2938. doi: 10.5194/bg-11-2925-2014

Mclachlan, A. J., and Cantrell, M. A. (1976). Sediment development and its influence on the distribution and tube structure of *Chironomus plumosus* L. (Chironomidae, Diptera) in a new impoundment. *Freshwater Biology* 6, 437–443. doi: 10.1111/j.1365-2427.1976.tb01632.x

Murniati, E., Gross, D., Herlina, H., Hancke, K., and Lorke, A. (2017). Effects of bioirrigation on the spatial and temporal dynamics of oxygen above the sediment-water interface. *Freshwater Sci.* 36, 784–795. doi: 10.1086/694854

Nepf, H. M. (2012). Flow and transport in regions with aquatic vegetation. *Annu. Rev. Fluid Mech. Fluid Mech.* 44, 123–142. doi: 10.1146/annurev-fluid-120710-101048

Nogaro, G., and Steinman, A. D. (2014). Influence of ecosystem engineers on ecosystem processes is mediated by lake sediment properties. *Oikos* 123, 500–512. doi: 10.1111/j.1600-0706.2013.00978.x

Oliveira Junior, E. S., Temmink, R. J. M., Buhler, B. F., Souza, R. M., Resende, N., and Spanings, T., et al. (2019). Benthivorous fish bioturbation reduces methane emissions, but increases total greenhouse gas emissions. *Freshw. Biol.* 64, 197–207. doi: 10.1111/fwb.13209

Peacock, M., Audet, J., Bastviken, D., Cook, S., Evans, C. D., and Grinham, A., et al. (2021). Small artificial waterbodies are widespread and persistent emitters of methane and carbon dioxide. *Glob. Chang. Biol.* 27, 5109–5123. doi: 10.1111/gcb.15762

Peters, V., and Conrad, R. (1996). Sequential reduction processes and initiation of CH4 production upon flooding of oxic upland soils. *Soil Biol. Biochem.* 28, 371–382. doi: 10.1016/0038-0717(95)0 0146-8

Pinheiro, J., Bates, D., DebRoy, S., Sarkar, D., Heisterkamp, S., van Willigen, B., et al. (2017). *Package 'nlme.' Linear and Nonlinear Mixed Effects Models, Version*, 3.

Poindexter, C. M., Baldocchi, D. D., Matthes, J. H., Knox, S. H., and Variano, E. A. (2016). The contribution of an overlooked transport process to a wetland's methane emissions. *Geophys. Res. Lett.* 48, 6276–6284. doi: 10.1002/2016GL068782

R Core Team. (2013). *R: A Language and Environment for Statistical Computing.*

Rosentreter, J. A., Borges, A. V., Deemer, B. R., Holgerson, M. A., Liu, S., and Song, C., et al. (2021). Half of global methane emissions come from highly variable aquatic ecosystem sources. *Nat. Geosci.* 14, 225–230. doi: 10.1038/s41561-021-00715-2

Roskosch, A., Hette, N., and Hupfer, M. (2012). Alteration of Chironomus plumosus ventilation activity and bioirrigation-mediated benthic fluxes by changes in temperature, oxygen concentration, and seasonal variations. *Freshw. Sci.* 31, 269–281. doi: 10.1899/11-043.1

Saunois, M., Stavert, A. R., Poulter, B., Bousquet, P., Canadell, J. G., and Jackson, R. B., et al. (2020). The global methane budget 2000 – 2017. *Earth Syst. Sci. Data* 12, 1561–1623. doi: 10.5194/essd-12-1561-2020

Sawakuchi, H. O., Bastviken, D., Sawakuchi, A. O., Ward, N. D., Borges, C. D., and Tsai, S. M., et al. (2016). Oxidative mitigation of aquatic methane emissions in large Amazonian rivers. *Glob. Chang. Biol.* 22, 1075–1085. doi: 10.1111/gcb.13169

Segers, R. (1998). *Methane Production and Methane Consumption: A Review of Processes Underlying Wetland Methane Fluxes*. Berlin: Springer. p. 41, 23–51.

Stadmark, J., and Leonardson, L. (2005). Emissions of greenhouse gases from ponds constructed for nitrogen removal. *Ecol. Eng.* 25, 542–551. doi: 10.1016/j.ecoleng.2005.07.004

Stehle, S., Manfrin, A., Feckler, A., Graf, T., Joschko, T. J., and Jupke, J., et al. (2022). Structural and functional development of twelve newly established floodplain pond mesocosms. *Ecol. Evol.* 12, 1–15. doi: 10.1002/ece3.8674

Thottathil, S. D., Reis, P. C. J., del Giorgio, P. A., and Prairie, Y. T. (2018). The extent and regulation of summer methane oxidation in Northern Lakes. *J. Geophy. Res. Biogeosci.* 123, 3216–3230. doi: 10.1029/2018JG004464

Walter, K. M., Smith, L. C., and Chapin, F. S. (2007). Methane bubbling from northern lakes: Present and future contributions to the global methane budget. *Philos. Trans. R. Soc. A Math. Phy. Eng. Sci.* 365, 1657–1676. doi: 10.1098/rsta.2007.2036

Yavitt, J. B., Angel, L. L., Fahey, T. J., Cirmo, C. P., and Driscoll, C. T. (1992). Methane fluxes, concentrations, and production Adirondack beaver impoundments. *Limnol. Oceanogr.* 37, 1057–1066. doi: 10.4319/lo.1992.37.5.1057

Zuur, A. F., Ieno, E. N., and Elphick, C. S. (2010). A protocol for data exploration to avoid common statistical problems. *Methods Ecol. Evol.* 1, 3–14. doi: 10.1111/j.2041-210X.2009.00001.x